QUASI-ELASTIC LIGHT SCATTERING FROM MIGRATING CHEMOTACTIC BANDS OF *ESCHERICHIA COLI*

MICHAEL HOLZ AND SOW-HSIN CHEN, *Massachusetts Institute of Technology, Cambridge, Massachusetts 02139 U.S.A.*

ABSTRACT We report the observation of migrating chemotactic bands of *Escherichia coli* in a buffer solution. The temporal development of the bacterial density profile is observed by the scattered light intensity as the band migrates through a stationary laser beam. We have made a preliminary analysis of the observed band profile with help of the Keller-Segel theory. The model accounts for only some aspects of the observed time evolution of the density profile. The microscopic motility characteristics of the *E. coli* in the band are simultaneously studied by photon correlation. The measured correlation functions are analyzed to obtain the spatial dependence of the half-width within the band. A simple analytical model is proposed to account for the contribution of the twiddle motion to the correlation function. By analyzing the correlation function as a superposition of straight-line and twiddle motions, we obtain a satisfactory agreement between the theory and the measured angular dependence of the line shape. As a consequence we are able to extract a parameter β, which measures the average fraction of twiddling bacteria in the center of the band at a given time.

INTRODUCTION

The chemotactic response of motile bacteria has attracted considerable interest. The main reason is that the study of molecular biological mechanisms responsible for the bacterial response to environmental stimuli may lead to the understanding of general principles involved in the molecular biology of sensory systems (1–3).

Microscopic motions of *Escherichia coli* have been particularly well studied in recent years. Analysis of movements of individual cells from stroboscopic photomicrographs (4) and especially by the tracking microscope (5) has lead to a "two-state" characterization of the bacterial motility. A cell is either "running" on a fairly straight path, or it is interrupted by a "twiddle," followed by another run in a nearly randomly chosen new direction. In a homogeneous medium the twiddles occur with constant probability. In the case of chemotaxis the random walk of the bacterium is biased by a change in the frequency of twiddles (1–3). Twiddles are less likely to occur for a run in a favorable direction, and thus on the average a net displacement of the cell results in that direction.

For a study of environmental effects on the chemotactic behavior of bacteria it is necessary to monitor changes in the frequency of twiddles quantitatively as a function

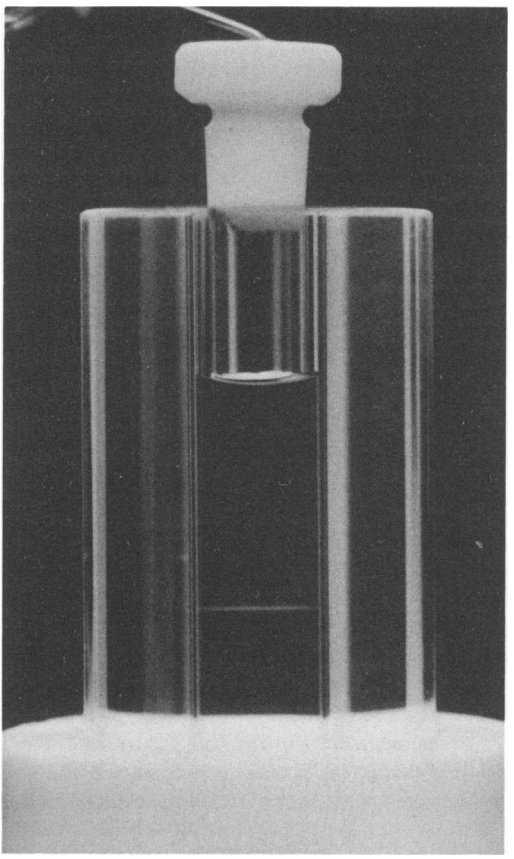

FIGURE 1 Migrating chemotactic band of *E. coli* in motility buffer. The sample is prepared by carefully layering a bacterial suspension on the bottom of the scattering cell, which is open to air. Band formation occurs after about 1 h. Typically, the well-defined bands migrate with an average speed of 0.3–0.7 μm/s until the meniscus is reached.

of the external perturbation. Such effects are difficult to detect with a single bacterium; instead a statistical analysis of many cells is necessary. Effects of the chemotactic response may also be studied by noting that the detailed microscopic motion of bacteria can result in a well-defined macroscopic manifestation. (6–9).

Under suitable conditions *E. coli* can form a slowly migrating, clearly visible sharp band (see Fig. 1). The striking phenomenon was first observed by Beyerinck (6). Careful studies by Adler (7) confirmed Beyerinck's interpretation that the formation and subsequent migration of the band is a consequence of the bacteria seeking an optimal oxygen concentration. The metabolic activity of the cells creates a traveling oxygen gradient, which the bacteria follow collectively. Only chemotactic bacteria can form a band. Adler and Dahl (8) provided a first clue to the molecular mechanism of the chemotaxis of *E. coli* by observing that methionine-starved cells cannot form a migrating band.

The migrating band is not the only example of collective behavior in a bacterial population. Bacteria innoculated on an agar plate can form clearly visible, slowly expanding rings (9). A redistribution of bacteria has also been observed when a perturbing step-gradient is introduced in an initially homogeneously distributed bacterial sample (10, 11). These experiments and corresponding theoretical models have been summarized by Boon (12).

In this article we study the temporal development of a migrating band by simultaneous measurements of the scattered light intensity and the intensity autocorrelation function. The experimental setup and sample preparation are described in Methods. Under Temporal Development of the Migrating Band the measured bacterial density distribution is compared with the predictions of a phenomenological model proposed by Keller and Segel (13). Then we show experimental evidence that the observed decay of the correlation function is sensitive to the average frequency of bacterial twiddles. To substantiate this conjecture, we develop a simple analytical model to account for the twiddle state of bacteria in light scattering. The predictions of this model are in good agreement with the scattering angle-dependence of the line shape of the correlation function. We conclude the paper by pointing out some possible further studies that might test the current microscopic picture of the chemotactic response of *E. coli*.

METHODS

Sample Preparation

Wild-type *Escherichia coli* K_{12} bacteria are grown in L-broth for 15 h at 30°C without shaking. To prepare a migrating band, the scattering cell (vol 1 ml) is first rinsed and filled with motility buffer (14) (10^{-2} M KPO_4, pH 6.9, 10^{-4} M EDTA, and 10^{-6} M L-methionine). Then 100 μl of the culture medium is carefully layered at the bottom of the scattering cell, which is left open to air. After 30–60 min a band of highly motile bacteria appears, as shown in Fig. 1. Band formation occurs with as little as 50 μl of added bacterial suspension.

After formation of the band, we pointed a laser beam into the center of the band, in the regions above and below the band, and finally near the bottom of the cell. A detector was placed at a suitable angle to detect the scattered light. The region below and above the band was found to be virtually free of any bacteria. The photon correlation function (15) obtained from the center of the band had an exceptional signal-to-noise ratio and exhibited a Gaussian line shape typical of self-propelled motion. Near the bottom of the cell we observed an exponential correlation function of much slower decay time, consistent with diffusive motion of the bacteria. These results can be qualitatively confirmed by microscopic examination of samples taken with a micropipette from respective regions in the cell. These observations are consistent with previously published works (6–8).

We have studied several such bands and find that a band generally ascends in the scattering cell until the meniscus is reached. There the band remains stationary and well defined and may be visible for up to several days, as was the case for the band reported here in the measurement of the scattering angle dependence. The band used in the measurement of the temporal dependence at fixed scattering angle, on the other hand, dispersed after approximately 5 h. It is interesting to note that in this particular case the motility buffer did not contain any methionine.

Scattering Setup

The photon correlation spectrometer is schematically shown in Fig. 2 and was similar to a setup previously used in this laboratory (16, 17). Laser light of wavelength 5,145 Å was focused by

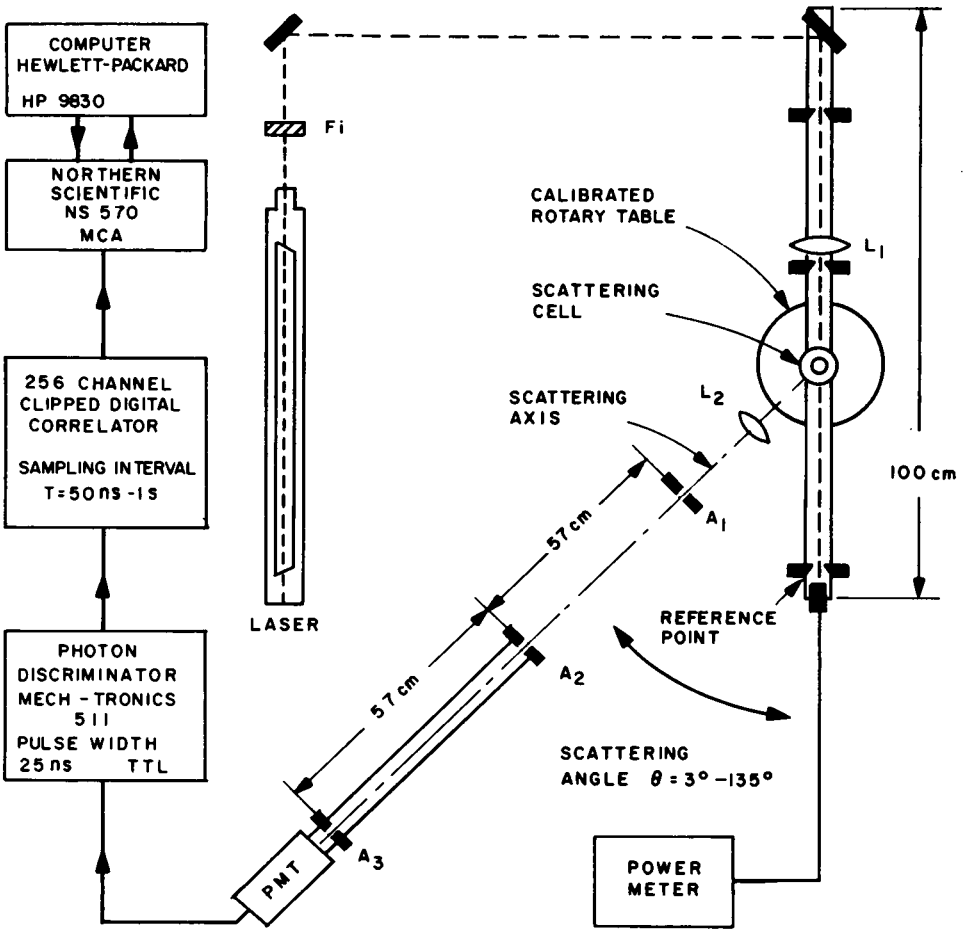

FIGURE 2 Photon correlation spectrometer.

lens L_1 (f = 209 mm) into the center of the cylindrical scattering cell made of quartz with 7 mm internal diameter and 1 ml volume (see Fig. 1). The waist of the focused beam had a diameter of 20 μm. Lens L_2 (f = 80 mm) imaged the scattered light on aperture A_1 (800 μm). Apertures A_2 (600 μm) and A_3 (400 μm) restricted the field of view of the photomultiplier tube to less than one coherence area. The scattering angle θ could be set continuously from 0° to 135° with 0.1° precision by means of a calibrated rotary table. A set of neutral density filters was used for attenuating the incident intensity of the laser beam.

The 256-channel photon correlator was interfaced with a Hewlett-Packard 9830A calculator (Hewlett-Packard Co., Palo Alto, Calif.) via a Tracor Northern NS-570 multi-channel analyzer (MCA) (Tracor Northern, Middleton, Wis.). The calculator timed the length of measurement, stored the accumulated correlation function and other pertinent data, such as scattering angle, sampling time, etc., on magnetic tape, cleared and reset the MCA, and printed a record of the experiment. On line, an estimate of the half-width of the correlation function was also provided by the calculator. The correlation function was accurately evaluated from the recorded data after the experiment.

Data Analysis

The accurate analysis of the half-width of a correlation function starts with an extrapolation of the correlated counts to zero delay time. To minimize the influence of statistical noise in the data, we extrapolated on several subsets of the first 15 delay channels by least-square-fitting each set to a parabola. We took the zero delay value as the mean of all extrapolations with negative curvature and 1 SD as a measure for the accuracy of the extrapolated point. Because the background was accurately measured by four monitor channels at an extended delay time, the uncertainty in the half-width was primarily determined by the error of the zero delay point. After subtraction of the background, the square roots of the data were taken to yield the field correlation function from the intensity correlation function, and the channel closest to the half-width was determined. The actual half-value was then found from a 20-point cubic least-square fit centered about the approximate half-point channel number.

TEMPORAL DEVELOPMENT OF THE MIGRATING BAND

Light scattering offers a unique capability for studying both the microscopic motility as well as the macroscopic temporal development of the band. If initially the laser beam is positioned above the band, as shown in Fig. 1, the very motion of the migrating band offers a sensitive scanning of the band profile with high temporal and spatial resolutions. The diameter (20 μm) of the laser beam going through the center of the scattering cell is much smaller than the thickness of the band (approximately 1 mm). The total intensity scattered by the bacteria at a fixed scattering angle was recorded on a strip-chart recorder to yield the bacterial density distribution as a function of time. Simultaneously, the temporal intensity fluctuations due to movements of the bacteria were measured. An accurate correlation function could be accumulated and stored in a time interval of 1–2 min. Since the band passed through the laser beam in about 30 min, approximately 10–20 correlation functions could be recorded at respective positions in the band. Thus the measured macroscopic density distribution was complemented by information on the microscopic motions averaged over all illuminated particles.

Bacterial Density Distribution

With this technique the temporal development of several migrating bands was observed. The strip-chart recording of one such band is shown in Fig. 3. For the measurement the scattering angle was chosen at 30°, and the incident laser power was approximately 0.15 mW. The ordinate represents the average count rate (time constant 5 s) on an arbitrary, linear scale and is directly proportional to the density of the bacteria. The abscissa marks the time in 5-min intervals. The relative position and time of the center of the bacterial density profile are denoted by X (millimeters) and T (minutes), respectively. During the $6\frac{1}{2}$ h of the experiment we observed five crossings of the laser beam by the migrating band.

An accurate value of the average speed of band migration can be estimated from the elapsed time between two successively recorded peaks in conjunction with the respective micrometer settings of the vertical translator of the scattering cell. The band of Fig. 3 migrated from position 1 to 2 with an average speed $\bar{v}$ = 40.8 μm/min = 0.68

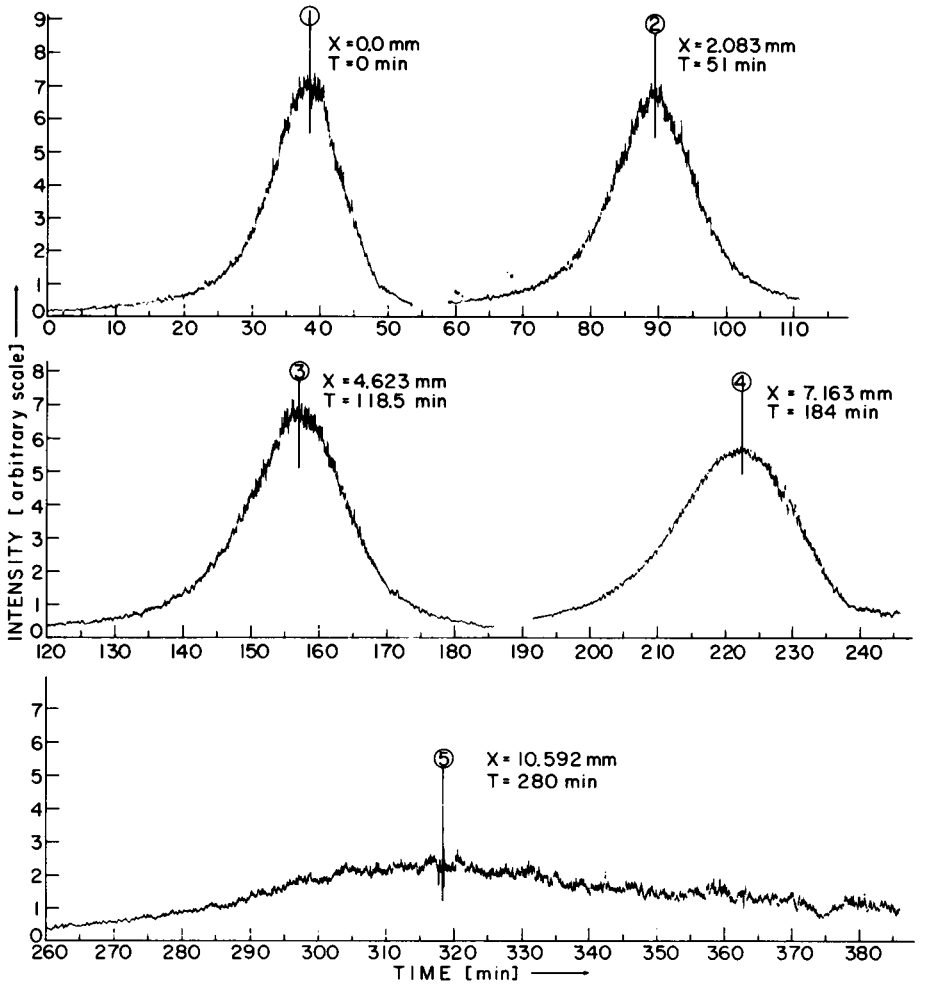

FIGURE 3 Temporal development of the migrating band. Scattered intensity at $\theta = 30°$ from a chemotactic band of *E. coli* migrating across a focused laser beam at fixed position. X and T give the relative position and time of successive peaks, respectively.

μm/s. For intervals 2–3, 3–4, and 4–5 the average speed is 37.6 μm/min, 38.8 μm/min, and 35.7 μm/min, respectively. The temporal variation of $\bar{v}$ introduces an apparent change of the band width on the strip-chart recording. The weak temporal dependence of the speed is approximated by a linear interpolation to convert each time point to a corresponding space point. The five density profiles are replotted in Fig. 4 on a spatially uniform scale. In this graph each curve may be approximately regarded as an "instantaneous" density distribution taken at roughly 1-h intervals. The area under each curve is proportional to the total number of bacteria in the band. Therefore it is clear that bacterial growth is minimal.

The density profiles of Fig. 4 are qualitatively reminiscent of the temporal change of the density distribution for Brownian particles in an external field (18). It is, in fact,

rather surprising to find a well-stabilized band configuration for the first 3 h. The band then disperses rather quickly. It clearly reflects a drastic change in the "behavior" of the bacteria after some interval of time. In the following, the Keller-Segel model of migrating bands will be sketched briefly and compared with the experimental observation on the migrating band.

The Keller-Segel Theory

Keller and Segel (13) have proposed a phenomenological model for the temporal development of a migrating band. They model the chemotaxis as resulting from a one-dimensional biased random walk. The bacteria take steps of constant length to the right or left at an average frequency depending on the concentration of a critical substrate. The model leads to a chemotactic force proportional to the gradient of substrate concentration and yields in the absence of growth the equation

$$(\partial/\partial t)b(x,t) = (\partial/\partial x)[\mu(\partial/\partial x)b(x,t) - \chi b(x,t)(\partial/\partial x)c(x,t)]. \quad (1)$$

The "chemotactic coefficient" $\chi(c)$ is a measure of the strength of chemotaxis. Eq. 1 must be supplemented with an equation for the rate of change of the substrate concentration, i.e.,

$$(\partial/\partial t)c(x,t) = -kb(x,t) + D(\partial^2/\partial x^2)c(x,t), \quad (2)$$

where $k(c)$ is the rate of consumption of substrate per cell, and D is the diffusion coefficient of the substrate.

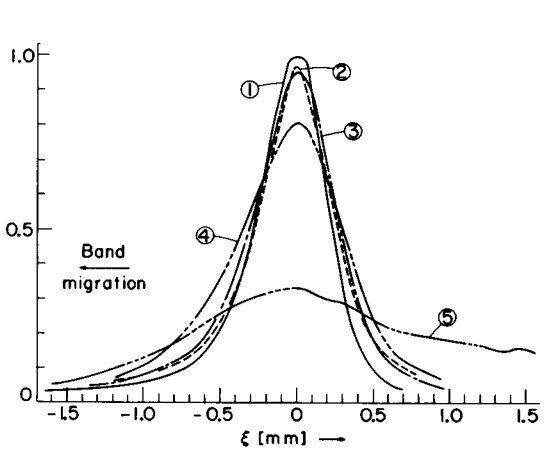

FIGURE 4

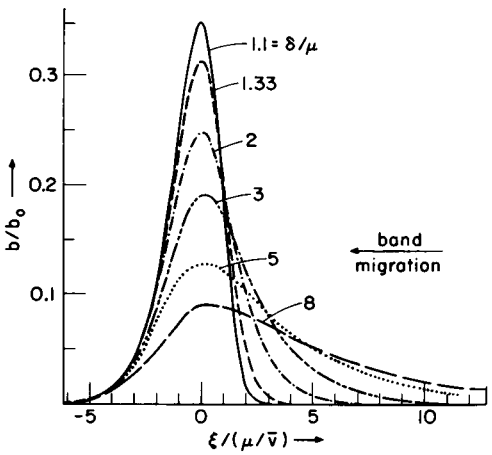

FIGURE 5

FIGURE 4 Bacterial density distribution in the migrating band. Bacterial density distribution of corresponding bands from Fig. 3 corrected for temporally varying speed of migration. The spatial position of each point is calculated by linearly interpolating the average speeds between three successive peaks.

FIGURE 5 Bacterial density distribution as predicted by the Keller-Segel model (13). Eq. 3 is evaluated for the indicated values of ratio δ/μ. The parameters δ, μ, and $\bar{v}$ are the chemotactic strength coefficient, the bacterial motility coefficient, and the average speed of the migrating band, respectively.

To solve Eqs. 1 and 2, Keller and Segel introduce the following assumptions (13): In Eq. 2 D is taken to be zero. The bacterial motility μ is assumed to be independent of concentration, in agreement with experimental observation (19), and k is taken as constant also. For the chemotactic strength coefficient $\chi(c)$, Keller and Segel tentatively use the form $\chi(c) = \delta/c$, where variable c now describes the deviation of the concentration from a certain threshold value. Boon (12) has pointed out that the last assumption actually changes the analytic form of the chemotactic force, which is now proportional to $\delta(\partial/\partial x \ln [c(x,t)]$.

The above assumptions together with the boundary conditions $b(x,0) = b_0$, $c(x,0) = c_0$, and $\partial/\partial x\, c(x,t) = (\partial/\partial x)b(x,t) = 0$ for $x = 0$ and $x = L \to \infty$ permit an analytic solution of the form $b(x,t) = b(\xi)$, $c(x,t) = c(\xi)$ where $\xi = x - \bar{v}t$. The bacterial density distribution can be written in the form

$$b(\xi)/b_0 = [\mu/(\delta - \mu)] \exp(-\bar{v}\xi/\mu)[1 + \exp(-\bar{v}\xi/\mu)]^{-\delta/(\delta-\mu)}, \quad (3)$$

with

$$b_0 = c_0\bar{v}^2/(k\mu),\ b_{max}/b_0 = (\delta/\mu)^{-\delta/(\delta-\mu)},$$

and

$$\bar{v} = kN/(Ac_0), \quad (4)$$

where N is the total number of bacteria in the band, and A the cross-sectional area of the sample cell. It is clear that a given number of bacteria deplete a larger section of a cuvette of smaller diameter and thus migrate faster in a thinner sample cell. The solution is valid only when $\delta > \mu$. Eq. 3 is plotted in Fig. 5 for several values of the ratio δ/μ.

Scribner et al. (20) have presented an extensive numerical study of Eqs. 1 and 2 with substrate concentration-dependent parameters and with $D \neq 0$. The calculated band profiles, in particular the bandwidth, are in quite close agreement to the prediction of Eq. 3. On the other hand, this more realistic treatment features a small but persistent loss of bacteria from the migrating band as evident from a gradual decrease of the height of the density distribution. This loss leads according to Eq. 4 to a change of the speed of migration to smaller values, in qualitative agreement with the experimental results as shown below.

Comparison with Experiment

The saturation concentration of oxygen in water (13) is $c_0 = 2 \cdot 10^{-4}$ mmol/ml and the area of the scattering cell is $A = 0.385$ cm^2. The total number of bacteria in the band is estimated as $N = 5 \cdot 10^6$ cells. The rate of oxygen consumption of *E. coli* is $k = 5 \cdot 10^{-12}$ mmol/cell h (13). With the above values the average speed is evaluated as $\bar{v} = 0.32$ cm/h $= 0.9$ μm/s. The agreement with the observed speed $\bar{v} = 0.6$ μm/s is not unreasonable, considering the rough estimates of the parameters. For a real test of Eq. 4 the parameters must be determined more accurately.

For a given motility μ the ratio δ/μ can be calculated from Eq. 3. Let us define the

width ξ of the band such that $b(\xi) = 0.1\ b_0$ with the respective $b(\xi)/b_{max}$ depending on the value of δ/μ as shown in Fig. 5. With $\delta/\mu = 1.33$ we find $b(\xi)/b_{max} = 0.32$, which corresponds to a width of $\xi = 0.4$ mm for the first three bands on the left side of Fig. 4. The average speed of migration in Fig. 3 from position 1 and 3 is found as $\bar{v} = 0.65$ μm/s = 0.23 cm/h. Taking the motility coefficient $\mu = 0.25$ cm^2/h as measured by Adler and Dahl (8) for *E. coli* yields from Eq. 3 a ratio $\delta/\mu = 1.42$. With these values for $\bar{v}$ and μ, the width is predicted (see Fig. 5) as $\xi = 2(\mu/\bar{v}) = 2.1$ cm, in contrast to the measured value $\xi = 0.4$ mm. The values of ξ and $\bar{v}$ are well defined experimentally, so we may try to adjust the motility coefficient to obtain a better agreement. If we choose $\mu = 5 \cdot 10^{-3}$ cm^2/h we have a width $\xi = 0.4$ mm and obtain a ratio $\delta/\mu = 1.72$. It is interesting to note that a value of $\mu = 2 \cdot 10^{-3}$ cm^2/h can be estimated (21) from the tracking results of Berg and Brown on *E. coli* (5).

The shape of the band profile, on the other hand, is in good agreement with the model. The calculated curves for ratio $\delta/\mu = 1.33$ in Fig. 5 are strikingly similar to the measured curves 1, 2, and 3. In particular, we observe the slightly slower rise of the density at the front end as compared to the back end of the band, predicted (13) for $\delta/\mu < 2$.

In summary, we may say that the simple analytical solution of the Keller-Segel model represents certain features of the migrating band reasonably. Nevertheless, some inconsistency exists with the experimental results. The model either predicts a density profile that is too broad or a speed of migration that is too high as compared to the experiment. The disagreement may be due to the assumption of $D = 0$ implicit in Eq. 3. In the numerical solution Scribner et al. (20) consider serine as substrate and use $D = 8.3 \cdot 10^{-6}$ cm^2/s, finding good agreement with the Keller-Segel solution. However, this value is still an order of magnitude slower than the diffusion coefficient of oxygen in water ($D = 2.12 \cdot 10^{-5}$ cm^2/s) (22). It appears interesting to recalculate the model for oxygen as a substrate or, alternately, to repeat the experiments with serine as substrate in order to test the Keller-Segel model adequately. The model also predicts a rather uniform thickness of the leading edge for all values of δ/μ. The experimental line shape, on the other hand, is fairly symmetric, and the leading edge shows variable thickness. Curve 5 appears asymmetric primarily because the band stopped migrating altogether. The bacteria disperse as expected for motile yet non-chemotactic bacteria (8). For such a situation the Keller-Segel model is obviously not applicable. In the next section it will be shown that the line width of the correlation function also reflects a dramatic change in the motility pattern for the bacteria in the bands.

TEMPORAL AND SPATIAL DEPENDENCE OF THE CORRELATION FUNCTION

In contrast to the macroscopic profile of the migrating band, the intensity autocorrelation function offers a microscopic description of the bacterial movements. The half-widths of the correlation functions (at 30° scattering angle) taken in the five bands shown in Fig. 3 are plotted in Fig. 6 as a function of position with respect to the center

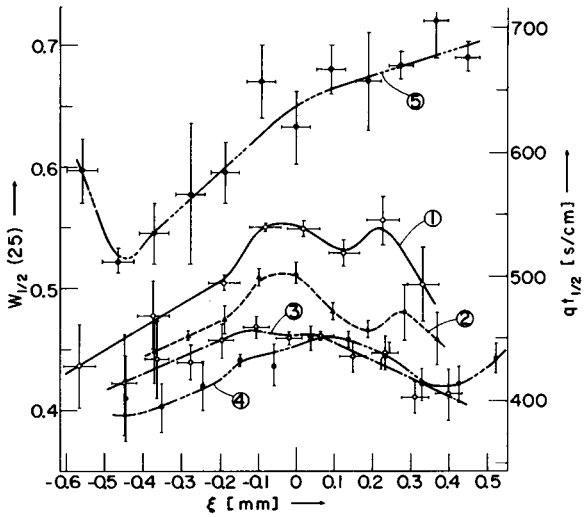

FIGURE 6 Spatial dependence of the half-width of $F_s(q, t)$ in the migrating band shown in Fig. 3.

of the density distribution. The conversion of line width $qt_{1/2}$ to $w_{1/2} \equiv qt_{1/2}\, u/\sqrt{6}$ is performed with an arbitrary reference speed $u = 25$ μm/s (assuming a Maxwellian speed distribution). The horizontal bars (shown only for curves 1, 3, and 5) signify the spatial spread of the measurement due to the finite time interval of data accumulation (2 min/run). The vertical error bars denote the uncertainty of the extrapolation to zero delay time for the correlation function. Near the wings of the density distribution the accuracy is reduced because of a smaller number of photons received per sampling interval. Points are shown only for cases in which the uncorrelated background amounts to at least 300 counts/channel. This threshold corresponds to a level of about 15% of the peak density. During one transit of the band through the laser beam, measurements of about 12 correlation functions can be made.

To guide the eye, points in Fig. 6 are connected by smooth lines. Bands 1–3 show a spatial dependence of the line width that is clearly above the uncertainty of individual points. Band 4 appears rather flat, and band 5 is strikingly different from the other cases. Before attempting to interpret these results in terms of a microscopic picture of the motion of the cell, we must convince ourselves that the observed spatial dependence of the line width is not due to multiple scattering.

Monochromatic light scattered by particles in motion is broadened to a spectral width $1/\tau_c$ in the frequency domain, where τ_c denotes the characteristic correlation time of the particle motion. When the scattered light is again scattered by another particle, the line width is further broadened to $2/\tau_c$. The time correlation function decays accordingly twice as fast, i.e., we expect a *narrowing* of the line width of the correlation function due to double scattering (23). The above argument is strictly true only when τ_c is independent of scattering angle. For bacteria this is not the case, as is shown later on (see Fig. 7). However, Eq. 9 can be used to estimate the effective line

width for all possible pairs of angles that add up to a given scattering angle ($\theta = 30°$ in this case). It is then found that multiple scattering leads still to a narrowing of the time correlation function.

Thus, as the band migrates into the beam, a gradual increase of multiple scattering can be expected to result in a decrease of the width of the correlation function. In contrast, the opposite effect is observed experimentally: the line width becomes wider near the center of the band. It must be concluded therefore that the spatial dependence of the half-width is not due to the multiple scattering, although multiple scattering may have actually weakened the observed change.

The dependence of the line shape as a function of position in the band can be qualitatively interpreted in terms of the microscopic motion of the bacteria. As mentioned in the Introduction, the *E.coli* seek an optimal oxygen concentration, less than the concentration found in water saturated with air at room temperature. The bacteria remain in the narrow band, because a departure from the region of optimal concentration at either side of the band induces an increased frequency of twiddles. The wings of the band are therefore populated with a larger fraction of twiddling bacteria. We shall show in the next section that a larger fraction of twiddling gives rise to a narrower correlation function. Thus it is consistent that the half-width decreases towards the wings of the bacterial distribution as shown in Fig. 6 (for curves 1–4).

The dramatic change of half-width for curve 5 further confirms this picture. When the band disperses, the bacteria must have lost their chemotactic ability, i.e., they are incapable of regulating the occurrence of twiddles (24). In fact, the bacteria may altogether lose the ability to twiddle. This seems to be what happens to the bacteria in band 5. The half-width is considerably broader, reflecting a much smaller fraction of twiddling bacteria. The gradual increase of the line width from left (earlier times) to right is due to a temporal change of the motility pattern that is convoluted with the spatial dependence.

A SIMPLE MODEL FOR THE CORRELATION FUNCTION OF BACTERIA IN THE TWIDDLE STATE

A successful quantitative interpretation of quasi-elastic light scattering data from a migrating band rests upon a correct model for predicting the observed line shape. Clearly, presence of a large fraction of twiddling bacteria should affect the line shape pronouncedly. None of the models proposed so far (25–28) take into account the presence of twiddling bacteria. In the following a simple analytical model for twiddling will be described.

Derivation

The motion of *E. coli* in the migrating band had been described by Adler and Dahl (8) as "very rapid, highly jerky motion" with short runs. On the stroboscopic microphotographs, as shown by Macnab and Koshland (4), the twiddling bacterium leaves a bright, smeared-out spot, i.e., the bacterial body jitters rapidly about an average location. By direct microscopic observation it can be clearly seen that the twiddling is

actually a rapid uncoordinated rotation. To capture the essence of this kind of motion, and yet to keep the model as simple as possible, the following assumptions will be made. Let us suppose that the center of mass of the twiddling bacterium jitters on a random path with step length l and velocity $\mathbf{v}(t)$. The direction of the velocity has an isotropic distribution and its random time dependence is approximated by a Gaussian random process. We assume also that the angular reorientation of the bacterium is so fast with respect to the decay time of the translational correlation function that the twiddling cell always appears spherically symmetric in the time scale of interest. Then the intermediate scattering function $F_s(\mathbf{q}, t)$, which describes the temporal decay of the field autocorrelation function, can be reduced into a form

$$F_s(\mathbf{q}, t) \equiv \left\langle \exp\left[i\mathbf{q} \cdot \int_0^t \mathbf{v}(t')\mathrm{d}t'\right]\right\rangle,$$

$$= \exp\left[-q^2 \int_0^t \mathrm{d}\tau(t - \tau)\langle v_z(0)v_z(\tau)\rangle\right]. \tag{5}$$

The $\langle\ \rangle$ brackets indicate average over all the bacteria. The scattering vector $\mathbf{q}$ points in the z-direction and has a magnitude $(4\pi/\lambda)n \cdot \sin(\theta/2)$ at scattering angle θ. The second expression follows from the first by expanding the exponential and noting that for a Gaussian random process all higher-order correlation functions of v_z can be reduced into products of two-time speed correlation functions. To proceed further, the temporal dependence of the speed autocorrelation function must be specified. The random directional change of a bacterium with average speed v_0 and step length l occurs on the average after a time $\tau_0 = l/v_0$. Thus a simple exponential decay of the autocorrelation function may be assumed, i.e.,

$$\langle v_z(0)v_z(\tau)\rangle = v_0^2 \exp(-\tau/\tau_0). \tag{6}$$

After substituting Eq. 6 into 5 and carrying out the time integration, we obtain the intermediate scattering function of bacteria in the twiddle state $F_1(q, t)$ as

$$F_1(q, t) = \exp\{-q^2l^2[t/\tau_0 - 1 + \exp(-t/\tau_0)]\}. \tag{7}$$

This expression is formally the same as the result obtained from the Langevin model (29) for the speed fluctuation.

The characteristic decay time of the intensity fluctuations is of order $(v_0q)^{-1} = \tau_0/(ql)$. In the large q limit where $ql \gg 1$, Eq. 7 is appreciable only for a range of time $t/\tau_0 \ll 1$. It is therefore well approximated by the expression: $F_1(q, t) \cong \exp(-\frac{1}{2}q^2v_0t^2)$. On the other hand, in the small q region where $ql \ll 1$ we need only to consider long times $t/\tau \gg 1$, and in this limit Eq. 7 reduces to: $F_1(q, t) \cong \exp(-q^2l^2t/\tau_0)$. It is seen that the magnitude of the parameter ql determines the shape of the functional decay. When $ql > 1$, the particle trajectory is a straight line over distances of the order q^{-1}, and we obtain a Gaussian correlation function characteristic of a free particle. In contrast, for $ql < 1$ the particle changes direction many times over the distance q^{-1} and behaves, as far as the light-scattering experiment is concerned, like a

Brownian particle leading to an exponential lineshape. Eq. 7 provides a description valid also for the intermediate case when $ql \sim 1$.

The correlation function of the scattered light contains contributions not only from the twiddling cells but from the "running" bacteria as well. To keep the model simple, the running state will be approximated by a straight line motion over distances much longer than q^{-1} with the effect of the form factor neglected (30). Then the intermediate scattering function $F_2(q, t)$ of bacteria in the running state has the form (31)

$$F_2(q, t) = \exp(-q^2u^2t^2/6), \tag{8}$$

where u is the rms speed of the Maxwellian swimming speed distribution.

In practice the decay time of the intensity correlation function is much shorter than the time which a bacterium spends on the average either twiddling or running. Since both kinds of motions are mutually exclusive, the respective contributions are additive. We are thus led to an intermediate scattering function of the form

$$F_s(q, t) = \beta F_1(q, t) + (1 - \beta)F_2(q, t), \tag{9}$$

where $F_1(q, t)$ and $F_2(q, t)$ are given by Eqs. 7 and 8, respectively.

The parameter β gives the fraction of bacteria that are twiddling. Let t_1 and t_2 be the amount of time which a typical bacterium spends in twiddling and running, respectively. For a given time T of measurement we can observe $T/(t_1 + t_2)$ twiddles of one bacterium, i.e., the total twiddle period is $t_1T/(t_1 + t_2)$. The fraction of bacteria twiddling is therefore $\beta = t_1/(t_1 + t_2)$.

Comparison with Experiment

The validity of the intermediate scattering function as given in Eq. 9 must be tested with a measurement of the angular dependence of the correlation function. The well-defined band considered here migrates during the first 5 h with an average speed of 0.38 μm/s. The migration eventually slows down to 0.23 μm/s shortly before the meniscus is reached, about 17 h after sample preparation. At each scattering angle the correlation function is accumulated for a period of 1 min. The measurement is repeated five times near the center of the band. The experiment is completed $4\frac{1}{2}$ h after sample preparation. Band motion is compensated by a vertical displacement of the scattering cell at each scattering angle θ. As shown before, the decay of the correlation function is only weakly dependent on position near the center of the band.

The half-width of $F_s(q, t)$ at the center of the migrating band is plotted in Fig. 7 as a function of scattering angle. Points are the average of five measurements and the bars denote 1 SD. The solid line is calculated from Eq. 9 with the following parameters: the average translational speed is found as $u = 22\ \mu$m/s; the twiddling bacteria jitter with a speed $v_0 = 55\ \mu$m/s and have a step length $l = 0.13\ \mu$m; the fraction of twiddling bacteria is $\beta = 0.67$. Eq. 9 is very sensitive to the specific choice of the parameters. Changing u to 23 μm/s, for example, results in a clearly poorer fit to the scattering angle dependence of the half-width. It is important to note that a unique set of

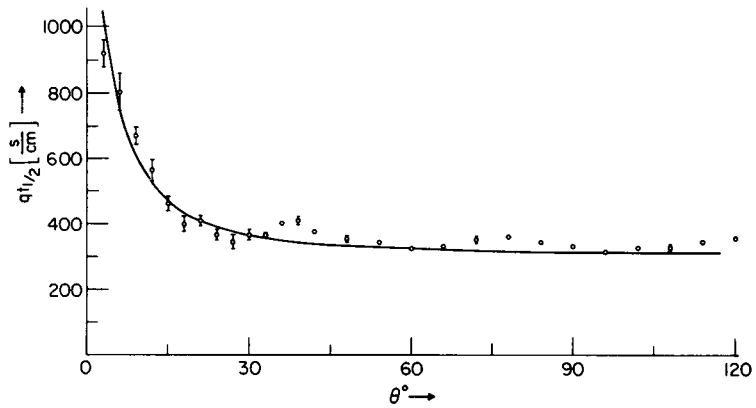

FIGURE 7 Scattering angle dependence of the half-width of the normalized field correlation function $F_s(q, t)$. Each experimental point is an average of five measurements and the bar denotes 1 SD. The solid line is calculated according to the model of twiddling and running bacteria as given in Eq. 9 with parameters: rms speed of running bacteria u = 22 μm/s; jitter speed of twiddling bacteria v_0 = 55 μm/s; step length of jitter motion l = 0.13 μm; and the average fraction of twiddling bacteria at a given time β = 0.67.

parameters can be determined only from a measurement at several scattering angles ranging from small to large.

The small deviations in the data points at around 40° and 80° indicate a contribution of the form factor (17), i.e., a factor that depends on the size, shape, and structure of the bacteria. This effect has been neglected in the present treatment but can be incorporated by choosing a more suitable form of the correlation function of bacteria in the running state (28).

Comparison of measured and calculated line shape at different scattering angles presents a more stringent test. Fig. 8 shows the measured intensity correlation function at four scattering angles. The time spectrum consists of a correlated time-dependent part and an uncorrelated background contribution. Here the background part is normalized to unity. Denoting the ratio of the correlated to uncorrelated signal by f, the measured intensity correlation function is related to the field correlation function by $(f | F_s(q, t) |^2 + 1)$. The line shape of curve 1 is calculated from Eq. 9 with the previous set of parameters. Curve 2 corresponds to the case when β = 0, i.e., when no twiddling bacteria are present. This line shape is expected for purely straight-line-swimming spheres and scales in the variable qt. It is evident that the simple model as given in Eq. 9 represents the measured data remarkably well.

CONCLUSION

The model described above offers the possibility of extracting from the correlation function the average fraction of bacteria that are twiddling at a given time. The value β is in accord with the visual observation that the bacteria in the migrating band are twiddling extensively. The absolute value of β, however, depends on the particular

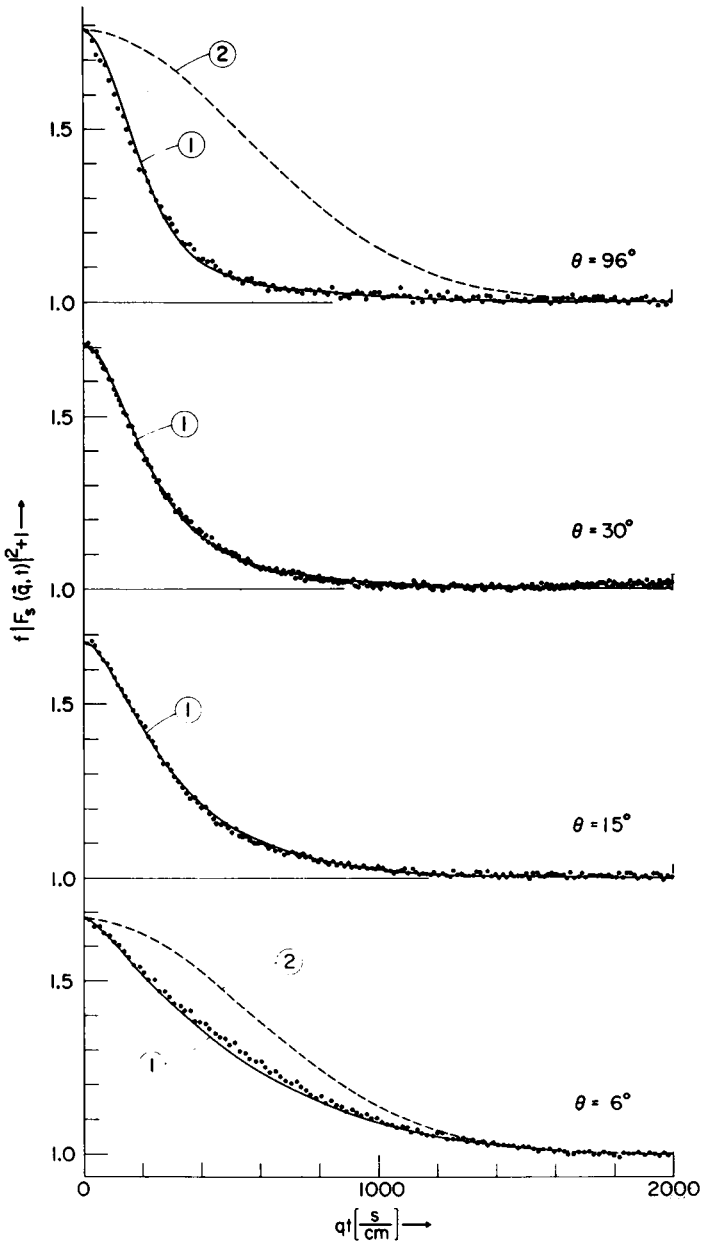

FIGURE 8 Line shape of the intensity correlation function from the migrating band at four scattering angles. The solid curves marked 1 are calculated from the model of Eq. 9 with the same parameters as in Fig. 7. The dashed curves 2 show the correlation function of purely translating spheres obtained from Eq. 9 by letting $\beta = 0$. This line shape when plotted in qt is independent of scattering angle.

model chosen to describe the contribution of bacteria in the running state. When the influence of the form factor is taken into account (17, 30), and rotational-translational motions are considered (28), the width for swimming bacteria is narrower than the Gaussian line shape assumed here (28). This will result in a lower value of β. The point particle description of the running state, however, allows us to use the simple functional form of the correlation function amenable to quick curve fitting. Under the premise that the running state remains unaltered when environmental conditions are changed, the simple model as given in Eq. 9 could be used to detect changes in the chemotactic response by monitoring the parameter β. These effects are difficult to detect on experiments dealing with a single bacterium. A change in chemotaxis is better described by a parameter such as β that represents a property averaged over many bacteria.

We have presented a discussion which illustrates the potential of the methods outlined in the previous sections for a detailed study of chemotaxis. A migrating band can be subjected to various environmental changes. Further study of the time evolution of the density distribution and the microscopic parameters such as u and β extracted from the correlation function as a function of position (within a band) and time promises to offer a stringent test of the current microscopic picture of chemotactic response of *E. coli* (1–3).

We are grateful to the referees of this paper for many constructive criticisms and a useful suggestion for a future experiment.

This research was supported by The Sloan Fund for Basic Research.

Received for publication December 24 1977.

REFERENCES

1. ADLER, J. 1975. Chemotaxis in bacteria. *Annu. Rev. Biochem.* **44**:341.
2. BERG, H. C. 1975. Chemotaxis in bacteria. *Annu. Rev. Biophys. Bioeng.* **4**:119.
3. KOSHLAND, D. E. JR. 1977. A response regulator model in a simple sensory system. *Science (Wash. D.C.).* **196**:1055.
4. MACNAB, R. M., and D. E. KOSHLAND, JR. 1972. The gradient sensing mechanism in bacterial chemotaxis. *Proc. Natl. Acad. Sci. U.S.A.* **60**:2509.
5. BERG, H. C., and D. A. BROWN. 1972. Chemotaxis in *Escherichia coli* analyzed by three-dimensional tracking. *Nature (Lond.).* **239**:500.
6. BEYERINCK, M. W. 1893. Ueber Atmungsfiguren beweglicher Bakterien. *Zentralbl. Bakteriol. Parasintenkd.* **14**:827.
7. ADLER, J. 1966. Chemotaxis in bacteria. *Science (Wash. D.C.).* **153**:708.
8. ADLER, J., and M. M. DAHL. 1967. A method for measuring the motility of bacteria and for comparing random and non-random motility. *J. Gen. Microbiol.* **46**:161.
9. NOSSAL, R. 1972. Growth and movement of rings of chemotactic bacteria. *Exp. Cell. Res.* **75**:138.
10. DAHLQUIST, F. W., P. LOVELY, and D. E. KOSHLAND, JR. 1973. Quantitative analysis of bacterial migration in chemotaxis. *Nat. New Biol.* **236**:120.
11. NOSSAL, R., and G. H. WEISS. 1973. Analysis of a densitometry assay for bacterial chemotaxis. *J. Theor. Biol.* **41**:143.
12. BOON, J. P. 1975. Theoretical models for bacterial motion and chemotaxis. *Adv. Chem. Phys.* **29**:169.
13. KELLER, E. F., and L. A. SEGEL. 1971. Traveling bands of chemotactic bacteria: a theoretical analysis. *J. Theor. Biol.* **30**:235.

14. ADLER, J., and B. Templeton. 1967. The effect of environmental conditions on the motility of *Escherichia coli*. *J. Gen. Microbiol.* **46**:175.
15. CHEN, S.-H., and A. V. NURMIKKO. 1974. Photon correlation spectroscopy in biology. *In* Spectroscopy in Biology and Chemistry-Neutron, X-ray, Laser. S.-H. Chen and S. Yip, editors. Academic Press, Inc., New York. 377.
16. CHEN, S.-H., W. B. VELDKAMP, and C. C. LAI. 1975. Simple digital clipped correlator for photon correlation spectroscopy. *Rev. Sci. Instrum.* **46**:1356.
17. HOLZ, M., and S.-H. CHEN. 1978. Structural effects in quasi-elastic light scattering from motile bacteria of *E. coli*. *Appl. Opt.* In press.
18. CHANDRASEKHAR, S. 1943. Stochastic problems in physics and astronomy. *Rev. Mod. Phys.* **15**:1.
19. NOSSAL, R., and S.-H. CHEN. 1973. Effects of chemoattractants on the motility of *Escherichia Coli*. *Nat. New Biol.* **244**:253.
20. SCRIBNER, T. L., L. A. SEGEL, and E. H. ROGERS. 1974. A numerical study of the formation and propagation of traveling bands of chemotactic bacteria. *J. Theor. Biol.* **46**:189.
21. LOVELY, P. S., and F. W. DAHLQUIST. 1975. Statistical measures of bacterial motility and chemotaxis. *J. Theor. Biol.* **50**:477.
22. MCCABE, M., and T. V. LAURENT. 1975. Diffusion of oxygen, nitrogen, and water in hyaluronate solutions. *Biochim. Biophys. Acta.* **399**:131.
23. BEYSENS, D., A. BOURGOU, and G. ZALCZER. 1976. Spectral measurements of the depolarized scattered light from a binary mixture near its critical point. *J. Phys. (Paris).* **27**:C1-225.
24. SPRINGER, M. S., E. N. KORT, S. H. LARSEN, G. W. ORDAL, R. W. READER, and J. ADLER. 1975. Role of methionine in bacterial chemotaxis: requirement for tumbling and involvement in information processing. *Proc. Natl. Acad. Sci. U.S.A.* **72**: 4640.
25. BOON, J. P., R. NOSSAL, and S.-H. CHEN. 1974. Light-scattering spectrum due to wiggling motions of bacteria. *Biophys. J.* **14**:847.
26. SCHAEFER, D. W., G. BANKS, and S. S. ALPERT. 1974. Intensity fluctuation spectroscopy of motile micro-organisms. *Nature (Lond.).* **248**:162.
27. STOCK, G. B., and F. D. CARLSON. 1975. Photon autocorrelation spectra of wobbling and translating bacteria. *In* Swimming and Flying in Nature. Y.-T. Wu, C. J. Brokaw, and C. Brennen, editors. Plenum Publishing Corporation, New York.
28. HOLZ, M., and S.-H. CHEN. 1978. Rotational-translational models for interpretation of quasi-elastic light scattering spectra of motile bacteria. *Appl. Opt.* In press.
29. UHLENBECK, G. E., and L. S. ORNSTEIN. 1930. On the theory of the brownian motion. *Phys. Rev.* **36**: 823.
30. CHEN, S.-H., M. HOLZ, and P. TARTAGLIA. 1977. Quasi-elastic light scattering from structured particles. *Appl. Opt.* **16**:187.
31. NOSSAL, R., S.-H. CHEN, and C. C. LAI. 1971. Use of laser scattering for quantitative determinations of bacterial motility. *Opt. Commun.* **4**:35.